Petroleum and Coal

Article **Open Access**

Aeromagnetic Evaluation of Basement Topography and Structures in the Nigerian Sector of the Dahomey Basin and Southwest Region

Michael Oluwaseyi Falufosi[1], Olawale Olakunle Osinowo[2] and Sikiru A. Amidu[3]

[1] *Pan African University Life and Earth Sciences Institute, University of Ibadan, Ibadan, Nigeria*
[2] *Department of Geology, University of Ibadan, Ibadan, Nigeria*
[3] *Pan African University Life and Earth Sciences Institute, University of Ibadan, Ibadan, Nigeria*

Received May 28, 2021; Accepted November 18, 2021

Abstract

The petroleum prospect of the Nigerian sector of the Dahomey Basin is evaluated with high resolution aeromagnetic data. The aim is to delineate the basin topography, deduce the presence of sufficient thickness of sediments and identify the presence of subsurface structures that can form hydrocarbon trapping mechanisms. The total field data was subjected to noise filtering, anomaly transformation and enhancement, with a view of performing geologic discrimination of the subsurface, map rock lineaments and determine basement depths. Radially averaged power spectrum was used to evaluate the noise-signal amplitude-frequency range of the data, which assisted with noise and regional field removal with Butterworth filter. Data processing also include removal of the IGRF field, downward continuation and reduction to pole. Generation of the derivatives, analytic signal, Euler depth solution and lineament maps form the basis of geological and structural mapping, including evaluation of basin architecture. Depth estimates from the total field power spectrum range from less than 1 km to 12 km, while 3D Euler Deconvolution indicates depth to basement range from < 500 m in the northern zone and up to 6000 m in the southern region, with a NE-SW trending relatively shallow region of maximum depth of 1500 m separating the western Dahomey Basin from the Eastern Niger Delta. The presence of up to 3000 m thickness of sediments and presence of fractures whose reactivation can form traps, suggest the potential for untapped resources in the unexplored parts of the Nigerian sector of the Dahomey Basin.

Keywords: *Dahomey Basin; Basement topography; Structures; Lineaments; Derivatives.*

1. Introduction

The Dahomey Basin is a petroliferous basin and commercial hydrocarbon reserves have been discovered in the Keta (Ghana), Seme (Benin Republic) and Lagos (Nigeria) parts of the basin. The basin was previously abandoned due to the Niger Delta oil boom, but recent renewal of hydrocarbon exploration interests in the basin is due to depletion of the Niger Delta hydrocarbon reserve. Discovery of hydrocarbon deposits in commercial quantities off the coast of Lagos in Aje field (1996) and Ogo field (2013) has further lend credence to continued exploration activities in the basin. Resources of economic importance, which had also been the subject of exploration include limestones, phosphorites, ironstones, kaolinite clay and water [1-2].

The acquisition of high resolution magnetic data by the Federal Government of Nigeria over the entire country have opened up opportunities for comprehensive and advanced studies into the geology and economic potential of the Nigerian geologic terrain. Although, literatures abound on the application potential fields in basement and basin studies of Nigeria, these available data are yet to be fully explored and thus, still potentially valuable for further studies. On the Dahomey Basin area, airborne magnetic data are often processed and interpreted for lineament mapping and basement depths. There are magnetic interpretation works on small parts of the basin, such as [3-4], but this study aim to carry out a basin-wide study of the basement topography and structures, in order to evaluate the hydrocarbon potential of the basin.

2. Location and geology of the study area

The study area is located within longitude 2° 30′ E – 6° 00′ E and latitude 6° 00′ N – 7° 30′ N, in south-western Nigeria. The study area covers the eastern Dahomey Basin, referred to as the Nigerian sector of the Dahomey Basin. The study area stretches eastward into the western area of the Niger Delta Basin. The geologic map of the study area, which was produced from the surface expression of outcrops and sediments and published by the Nigerian Geological Survey Agency (NGSA) is presented in Figure 1. Precambrian Basement Complex rocks occupy the northern part of the study area, while sedimentary rocks occupy the southern parts. The chiefly granitic basement rocks terrain is highly fractured and has been described to be block faulted [5]. Basement subsidence during the Early Cretaceous resulted in the deposition of thick sequence of continental sediments [6]. The major Cretaceous sedimentary lithologies include sands, shales and limestones. The Tertiary to Recent sediments include sands, shales, limestones, mudstones and claystones [7-8]. The Cretaceous sands form outcrops around the basement boundary.

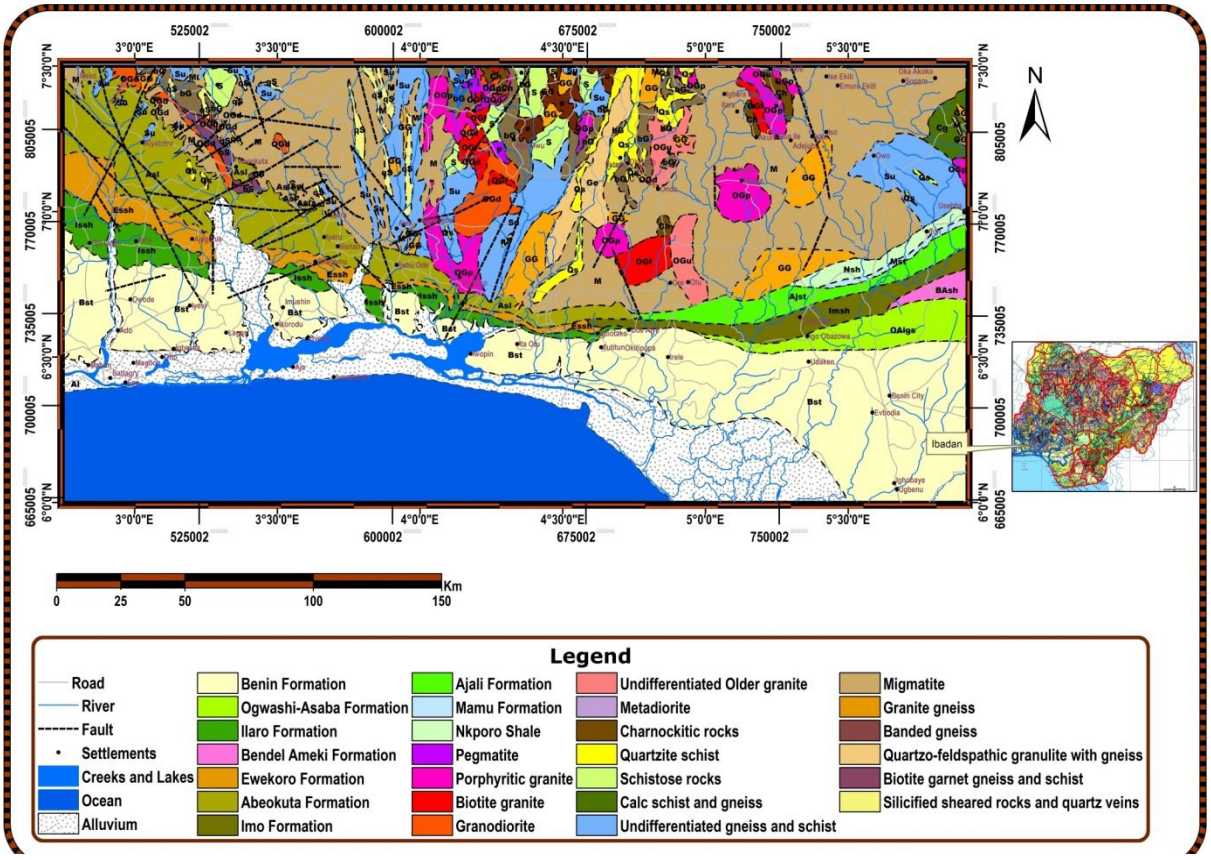

Figure 1. Geologic map of the study area

3. Methods

The datasets used include airborne magnetic data acquired from the Nigerian Geological Survey Agency (NGSA) and the ETOPO1 digital terrain models (DTM) acquired from the National Oceanic and Atmospheric Administration (NOAA). The aeromagnetic data was subjected to series of processing and anomaly enhancements using Oasis Montaj software.

3.1. The airborne magnetic data

The high resolution aeromagnetic data was acquired from the Nigerian Geological Survey. Data acquisitions were carried out with fixed wing Cessna aircrafts, with mean terrain clear-

ance of 80 m. Measurements were recorded at an interval of 0.1 seconds or less, which corresponds to station spacing of approximately 7 m. Flight lines spacing is 500 m with a trend of 135° (NW-SE), while tie lines spacing is 5000 m, with a trend of 45°. The pre-processed data was provided by the NGSA as a 2D grid of total magnetic intensity (TMI), with constant cell spacing of 100 m. The IGRF 2005 model was used in calculation of declination and inclination, since the data was collected from 2005 and 2009. The geographic coordinate system and WGS 84 reference datum were used during data acquisition and pre-processing. The coordinate system was however transformed to the UTM Zone 31N Cartesian coordinate system prior to processing.

3.2. Data analysis and processing

A value of 33,000 nT was added to the TMI data as this was removed initially from the field data during pre-processing. In order to correct for the flight height, the data was downward continued [9] to 80 m, which corresponds to the height of measurement aircraft above terrain. Butterworth lowpass filter was then applied, with a cut-off wavelength of 2000 m, which is 4 times the original line spacing of 500 m [10] to attenuate noise. Butterworth bandpass filtering was later applied after IGRF removal and reduction to pole, to obtain the residual anomaly data. The filter was implemented with long wavelength cut-off of 100 km and short wavelength cut-off of 5 km, thereby leaving the intermediate fields for further processing and anomaly enhancements.

3.2.1. Removal of the IGRF field

The IGRF (International Geomagnetic Reference Field) is used to compute a theoretical magnetic field of the earth. The resulting data from the subtraction of the IGRF field from the total field magnetic data is often referred to as IGRF Residual. The IGRF Residual is sometimes referred to as magnetic anomaly [9] and it is due to variation in magnetic intensity of crustal rocks, which is what is important in magnetic surveys. In this work, the acquired total field magnetic data is referred to as the commonly accepted total magnetic intensity (TMI), while the IGRF Residual is referred to as the total magnetic anomaly (TMA). The 2005 IGRF model was used for this work, since most of the data was acquired between 2005 and 2007.

3.2.2. Reduction to pole (RTP)

Reduction to pole transformation of the magnetic data was implemented to facilitate interpretations [10]. The operation affects both the amplitude and phase of the anomaly and transforms the data to that which would have been obtained at the magnetic pole [11], such that the direction of magnetization and ambient field are both vertical and symmetrical above the source body [12-13]]. The RTP process [14] involves Fourier transform of the data into the frequency domain and multiplication of the result by the RTP operator [15-18].

The standard RTP procedure assumes the direction of the earth magnetic field and crustal magnetization is constant. This may be plausible for small-scale local studies, but not valid for large-scale regional studies [19], in which magnetic inclination and declination changes significantly. In order to mitigate the problem, as the study area spans several degrees of longitude, the differential reduction to pole (DRTP) technique was implemented. The DRTP technique [19-21] is a modification of the RTP [14] technique and its purpose is to facilitate transformation of magnetic anomalies on a regional scale, spanning several degrees of latitude and longitude.

The RTP operator is an inverse function of inclination, and as inclination approaches zero, the filter becomes unstable [22-23]. This situation is prevalent around the equator and regions of low latitudes, within which the study area is located. This causes directional amplification of the anomalies and inherent noise [16,18,24]. There are several solutions to problem [25-28], directional filtering [26], but the implemented approach is the simple modification of the DRTP filter [17-18]. This involves the use of a modified inclination (I′ equals 20°) set greater than the true inclination (-12.7°).

3.2.3. Derivatives and analytic signal

Derivative filters were applied to the RTP data for delineation of edges and geological boundaries [29]. Horizontal (x and y) and vertical (z) derivatives are very sensitive to the edges of bodies and are thus called edge detectors. The total horizontal derivative is the vector sum of the horizontal (x and y) derivatives and peaks over vertical contacts or forms a ridge, if the source is narrow. The tilt derivative, which is the arctan of the ratio of vertical derivative to the total horizontal derivative was also calculated and it produces patterns that are similar to the first order vertical derivative [9]. Analytic signal grid was also generated from the RTP data and the result was used for structural and geologic discriminations. The analytic signal concept as used in this work is the 3D analytical signal amplitude or simply 3D ASA for short [30]. The analytic signal in 3-dimensions was given by [31], and it is essentially the vector sum of the horizontal (x and y) and vertical derivatives.

3.2.4. Centre for exploration targeting (CET) grid analysis

The CET grid analysis algorithm was developed by the Centre for Exploration Targeting (CET), based at the University of Western Australia. The algorithm, provided as a plugin in Oasis Montaj was used for lineament and edge detection. There are two tools available for lineament and edge detection. These include the Phase Symmetry, which enhances the appearance of linear features and Phase Congruency, which detects discontinuities or edges. Phase symmetry is used in detecting ridges/valleys, while phase congruency is used in detecting edges. Phase symmetry involves identifying axes of symmetry. At the point of symmetry the amplitudes of all frequency components of the data are at maximum, and the axis of symmetry is perpendicular to the orientation of the profile line. In order to identify points of symmetry in the 2D data, the data is first broken into 1D profiles and analyzed over multiple orientations at varying scales. Phase congruency depends on the fact that edge features occur at points where local frequency components are maximally in phase. At the edge points, all the component waves are in phase. The resultant solution plots are curves, which are then vectorized into straight lines. Lines less than 5 km in length were rejected.

3.2.5. Depth to Basement – Euler deconvolution

The conventional Euler deconvolution method of depth estimation was applied to the data [32], in order to determine the depth and location of the source body. It makes use of the three orthogonal (x, y and z) derivatives of the total magnetic intensity (TMI) data, the value of the regional magnetic field and a structural index (SI). The structural index (SI) depends on suspected geometry of the source body and values of 0 and 1 were used for contact and dyke models respectively [33-34].

The target depth range was 0 to 10,000 metres [4,35-40], and attempts were made to use various window size ranging from 2000 to 10,000 m [10,34,41-42]. In the initial calculations, the maximum percentage depth tolerance (dZ) is set at 25 %. The solutions were windowed (reduced) with variable parameters in order to eliminate spurious values. These include the maximum percentage depth tolerance or uncertainty (dZ), maximum percentage location tolerance or uncertainty (dXY) and maximum/minimum depth. The X-Offset and Y-Offset were also used to window the solutions. These represent the x and y distance of Euler solutions from the centre of the moving window. Solutions located farther than half the value of the solution window size are often not reliable [10].

The initial computation was done with a window size of 2000 m, and structural index of 0.0, for contact/fracture model. The solutions were windowed to dZ of 10 %, dXY of 15 %, X-Offset of +/- 1000 m and Y-Offset of +/- 1000 m. Upon scrutinizing the depth solutions with well depths, the solutions were discovered to be generally too shallow. The window size was increased to 4000 m, so that depths up to 8000 m could be accepted with a realistic level of confidence, as depths greater than twice the window size are generally deemed to be unreliable [34,41]. The accepted solutions thereafter was carried out with a structural index of 1.0 for dyke model and then windowed to dZ of 10 %, dXY of 15 %, X-Offset of +/- 2000 m and Y-

Offset of +/- 2000 m. The remaining solutions were dot plotted and also gridded. The elevation data used for topographic correction of the depth solutions is the ETOPO1 1-Arc Minute digital terrain model (DTM).

4. Results

Geologic and structural interpretations were initially carried out through qualitative interpretation. This is then followed up with quantitative interpretations, involving lineament mapping and 3D Euler calculation of source depths.

4.1. Total field magnetic anomaly distribution

The total magnetic intensity (TMI) values (Figure 2) range from 32000 to 34000 nT. The values generally decrease from north to south and from west to east. The northern half of the study area displays complexity in amplitude variations and has strong imprints of short wavelength anomalies. This area is dominated by basement rocks. The southern half is dominated by long wavelength anomalies and the relatively smooth appearance of this area suggests deeper magnetic sources. Magnetic intensity values are generally higher towards the basement terrain and the anomalies trend in an approximately NE-SW direction.

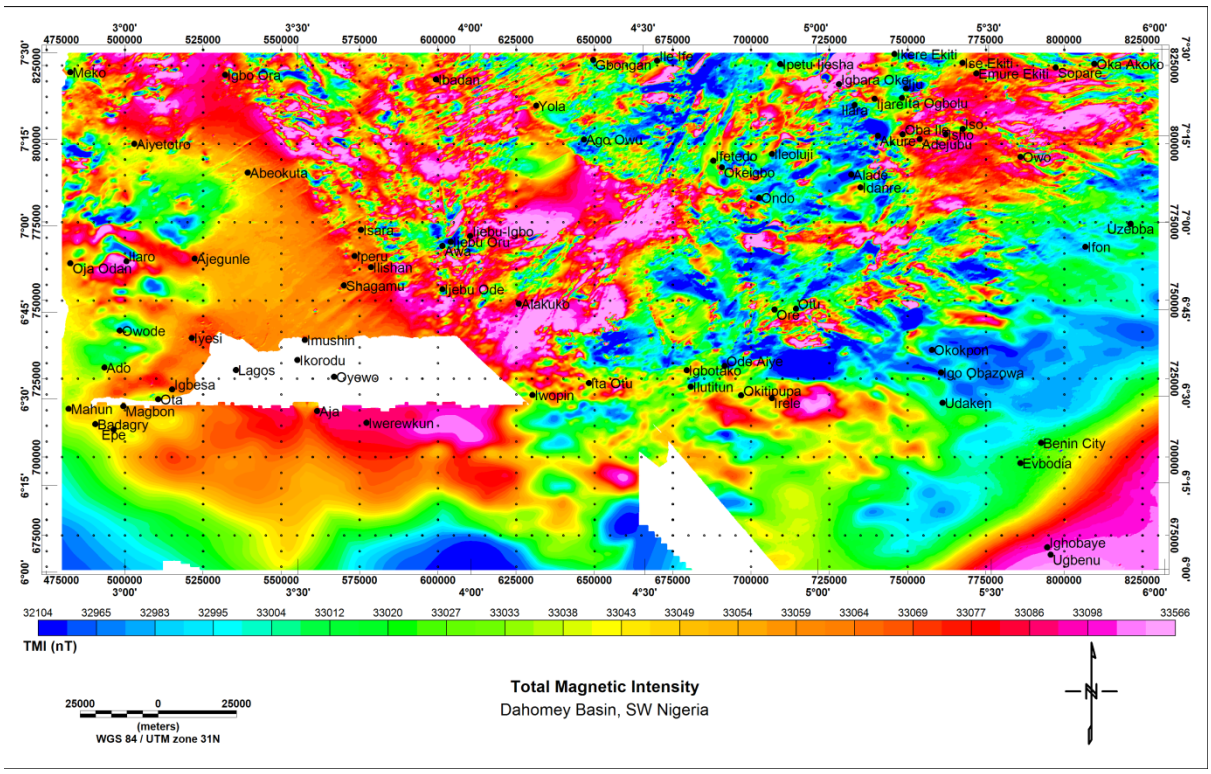

Figure 2. Total field magnetic intensity distribution

4.2. Reduction to pole at low latitude residual magnetic anomaly distribution

The reduction to pole residual magnetic anomaly values (Figure 3) range from -326 to 517 nT. Anomaly trends range from NW-SE in the western and eastern areas, to a predominantly NE-SW trend in the central area. A basement fracture of regional proportion exists around the centre of the study area. This is designated by a NNE-SSW trending negative anomaly (< -70 nT). The Dahomey Basin in south-west of the map shows anomaly values that decrease from east to west, from > 400 nT to < 20 nT. This, including the increasing smoothening of the anomalies in this direction suggests increasing basin depths. The eastern half of the study area is dominated by two NE-SW trending high positive (> 25 nT) anomalous zones, running from north to south, through the middle and eastern end of the map.

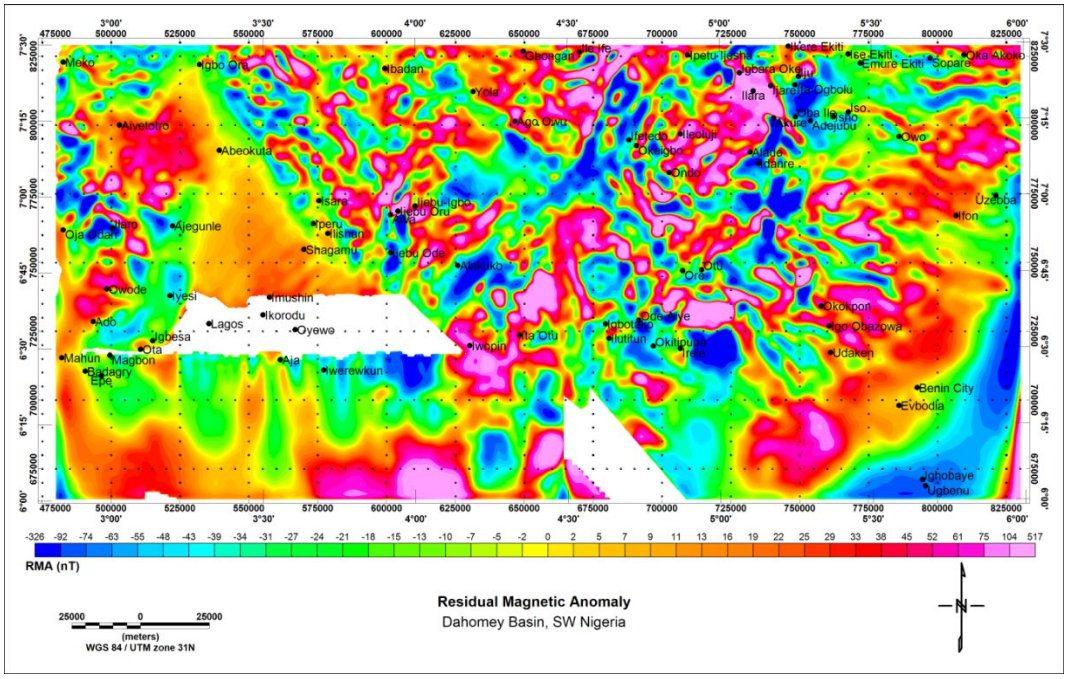

Figure 3. Pole reduced residual magnetic anomaly distribution

4.3. Horizontal derivatives of the magnetic data

The x-derivative map (Figure 4) indicates a general north-south trend of basement structures, but exact orientations vary considerably across the study area.

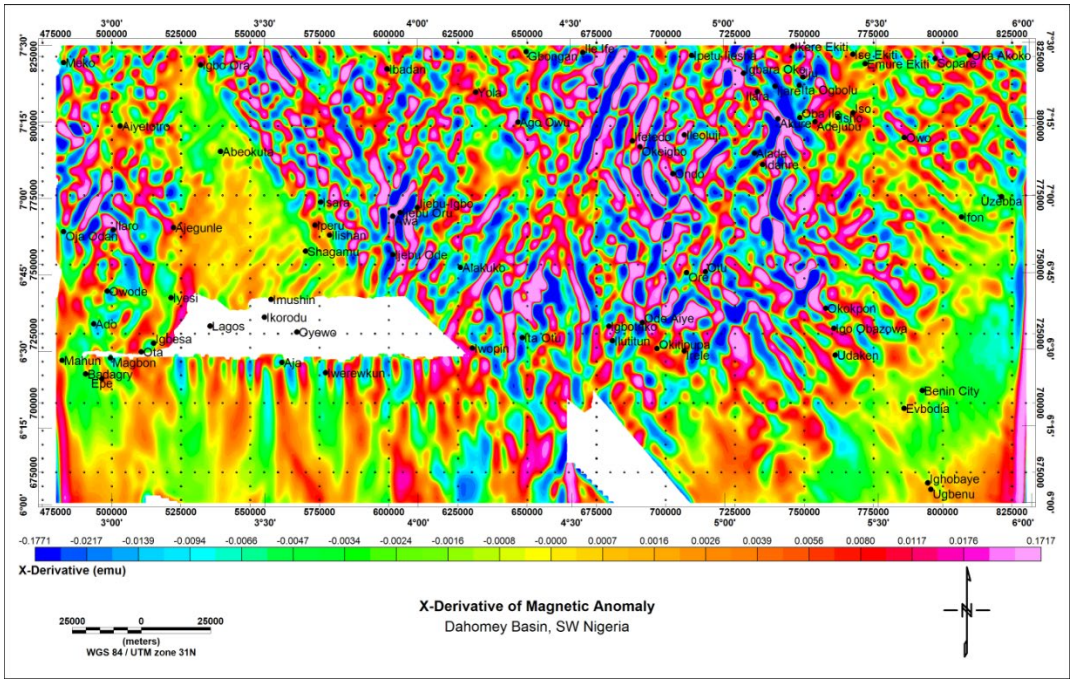

Figure 4. X-derivative of magnetic anomaly

Moving from west to east, the structures trend NE-SW in the western part, NW-SE / NE-SW in the central parts and NW-SE in the eastern part. The elongated features are not well defined in the southern parts but their general north-south trend visible. The y-derivative map (Figure 5) shows the general east-west trend typical of y-derivative maps. However, as the

Nigerian basement terrain have been established to have a general north-south trend, this result is only reliable in the regions where the trends are tilted northward, especially around the north-central areas.

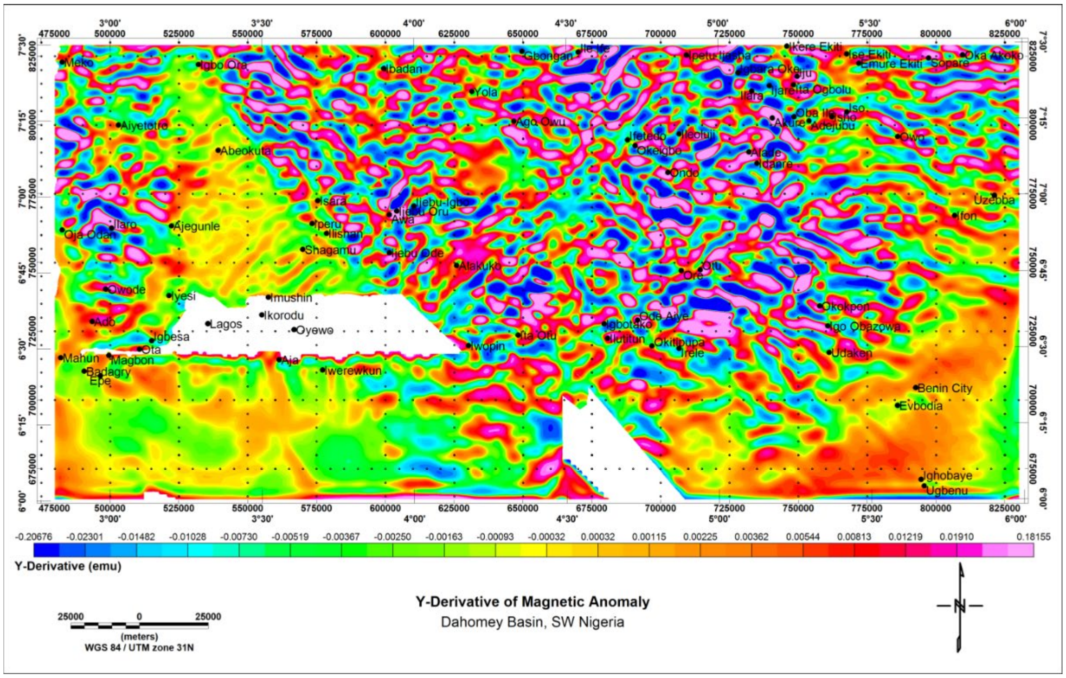

Figure 5. Y-derivative of magnetic anomaly

The total horizontal derivatives (Figure 6) produced results similar to that generated by the x-derivative. However, the total horizontal derivative is characterized with short-wavelength noise and relatively poorer contrast.

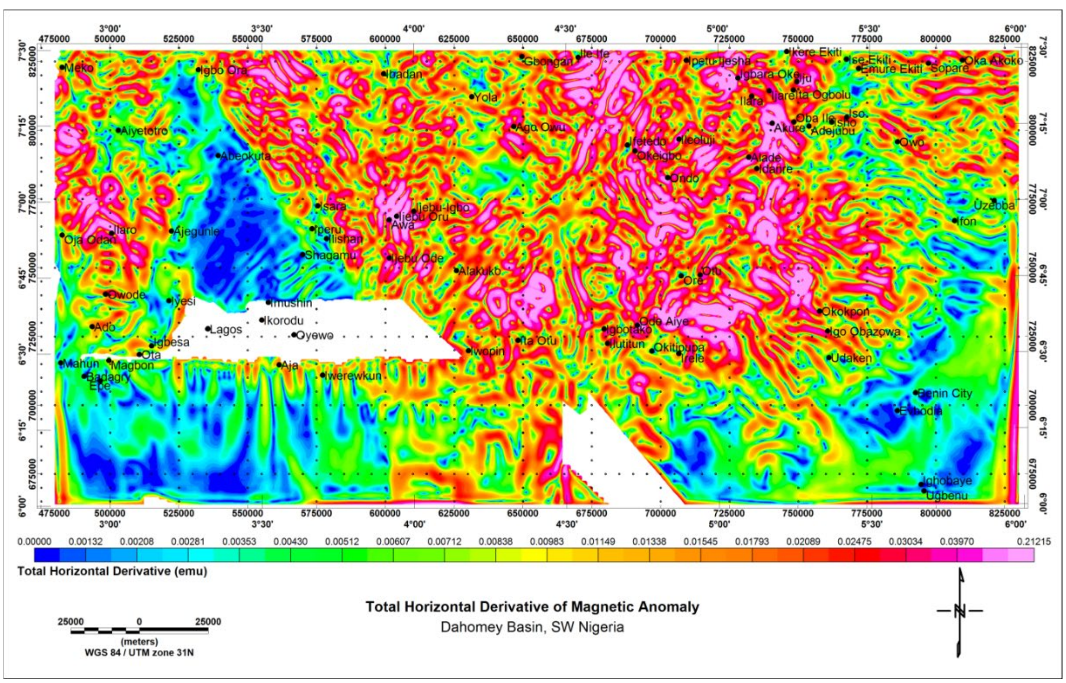

Figure 6. Total horizontal derivative of magnetic anomaly

However, the general north-south trend of anomalies are still visible, as well as the alternating nature of the structural trends from west to east. The Dahomey Basin in the south-

west of the study area is dominated by basement structures that trends almost north-south. This is different from the obvious NE-SW trend over the Niger Delta Basin in the south-east of the study area.

4.4. Vertical (Z) derivative of the magnetic anomaly data

The z-derivatives of the magnetic anomaly data is presented in Figure 7. The z-derivative is similar to the x-derivative, although the structures are relatively less continuous. However, they are well defined, with high anomaly contrasts. The predominantly north-south trending derivative anomalies are well defined in almost the entire part of the study area, although in the north, the terrain shows relatively better contrast. The structural is also observed to vary from west to east, with the north-western areas showing a predominantly NE-SW trend. In the basement terrain, the structural trends vary from west-east, from a predominantly NW-SE direction within the western parts, to a predominantly NE-SW trend in the central areas. The structural trend in the eastern parts is predominantly NW-SE, and the anomalies can be observed to extend from the sedimentary terrain in the south-east to the basement terrain in the north. The Dahomey Basin, located in the south-western part of the study area can be separated from the Niger Delta area by its conspicuous north-south trending anomalies.

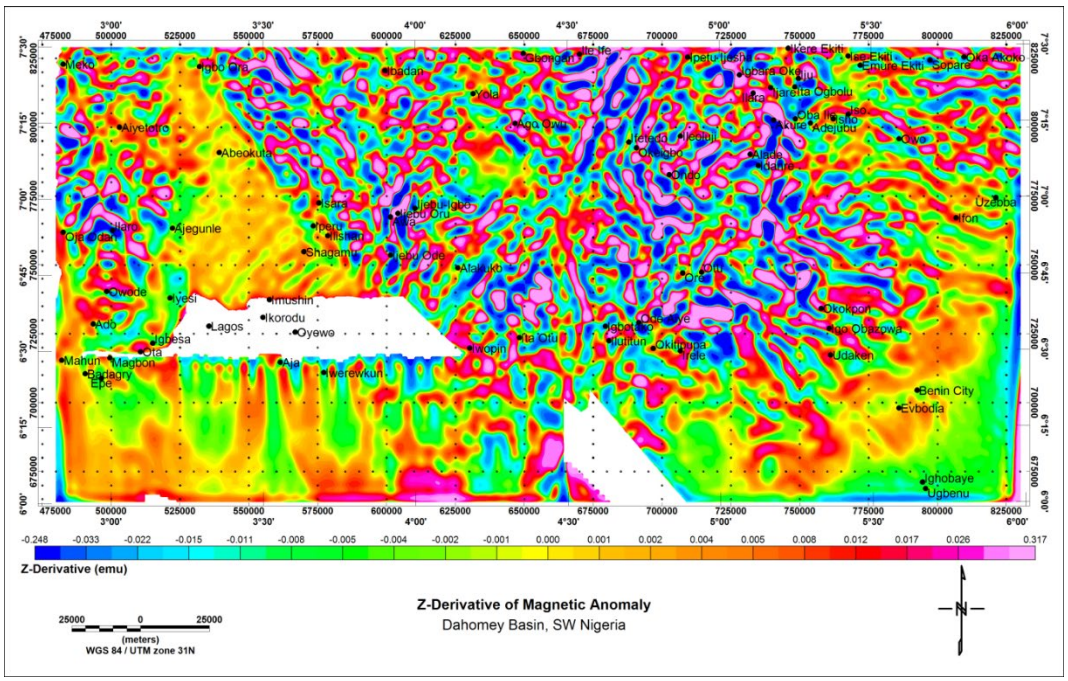

Figure 7. Z-derivative of magnetic anomaly data

4.5. Tilt derivative of the magnetic anomaly data

The tilt derivatives map of the study area, extracted from the magnetic anomaly data is presented in Figure 8. The tilt derivative produces similar results as the vertical derivative, with the major difference being that in the tilt derivative map, the anomalies are narrower. As a result, the peaks are better placed over the subsurface discontinuities, thereby facilitating a relatively more accurate mapping. The general north-south trend of the basement rocks and the changing orientations from west to east are vividly visible. Several fractures of significant proportions can be traced on the map. A NE-SW trend negative anomaly trace is observed to run through the middle of the map. This corresponds to the well-known regional Ifewara-Zungeru fracture [43]. Several other fractures of varying proportions are observed in the northwestern and northeastern parts of the study area. The fractures generally trend in the NW-SE direction.

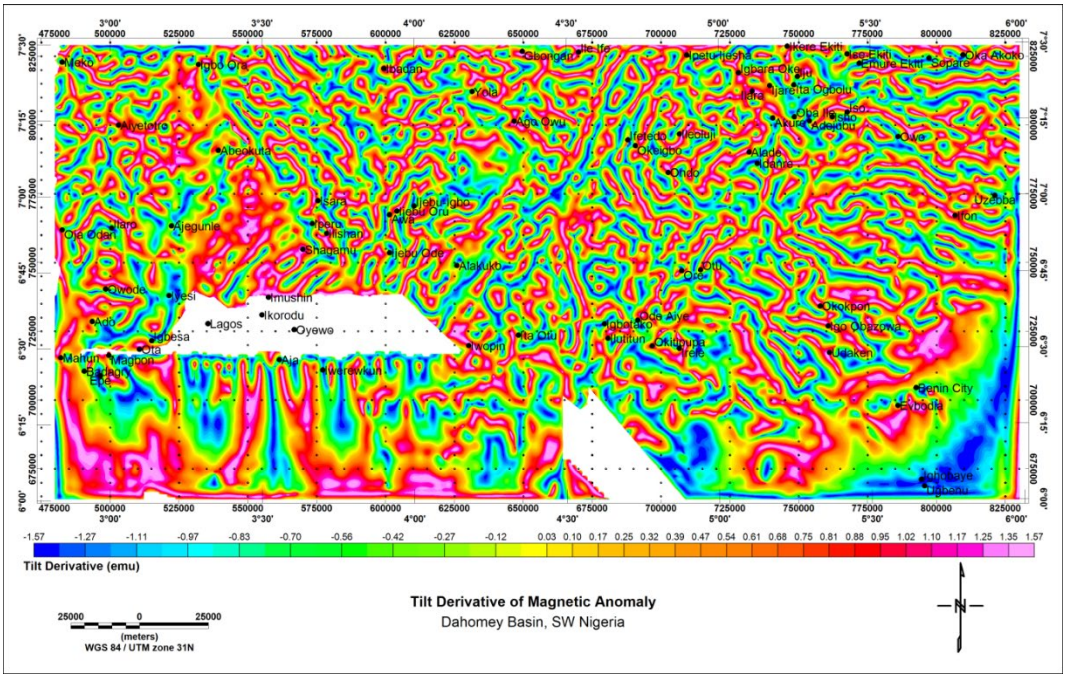

Figure 8. Tilt derivative of magnetic anomaly data

4.6. Analytic signal of the magnetic anomaly data

The analytic signal map generated from the magnetic anomaly data is presented in Figure 9.

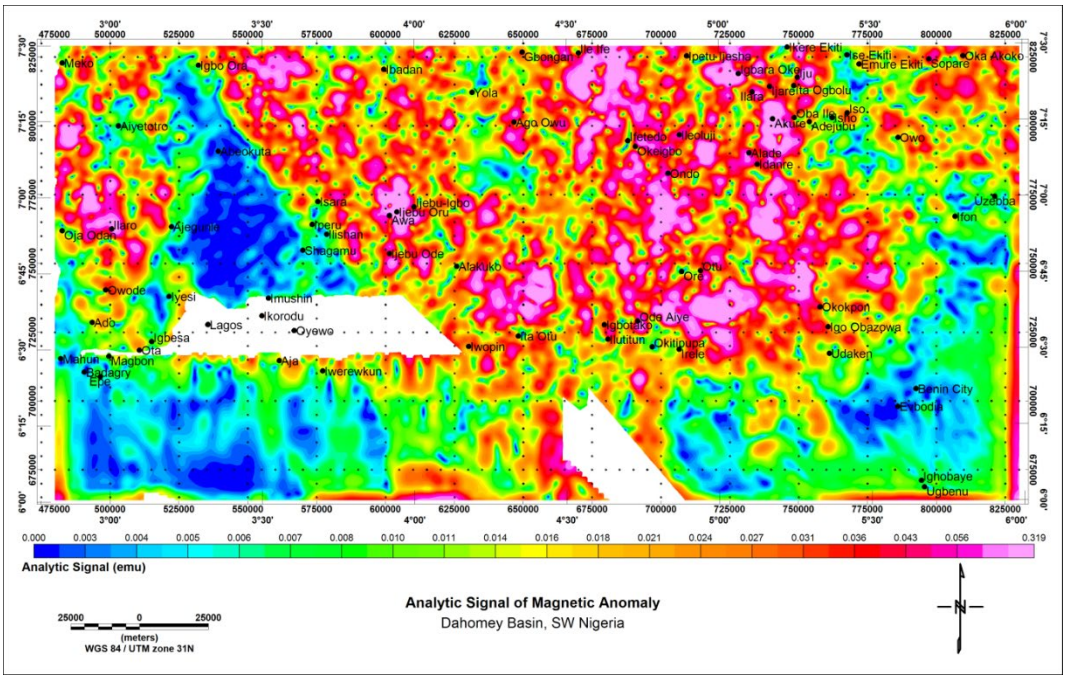

Figure 9. Analytic signal of the magnetic anomaly data

This enables the characterization of the geologic terrain into basement and sedimentary terrains, and also separates the Dahomey Basin from the Niger Delta. High positive (> 0.03 emu) anomaly amplitudes dominate the basement terrain which occur north of the study area. The anomalies terminate in the transition zones. The Dahomey Basin in the south-western region is dominated predominantly by low amplitude (< 0.01 emu) anomaly signatures. However, the area can be conveniently divided to two parts; the western part, dominated by low

amplitude (< 0.0005 emu) anomalies and the eastern part, dominated by anomaly amplitudes ranging from 0.007 – 0.014 emu. A region of high amplitude (> 0.024 emu) anomalies separates the Dahomey Basin from the predominantly low anomaly amplitude (< 0.01) dominated Niger Delta Basin in the south-east end of the study area.

4.7. CET lineament analysis of magnetic data

The edge solutions (Figure 10) are best developed in the basement terrain, but poorly developed in the southern parts. The lineaments have a predominant north-south direction, but the earlier identified variation in structural trends is well defined.

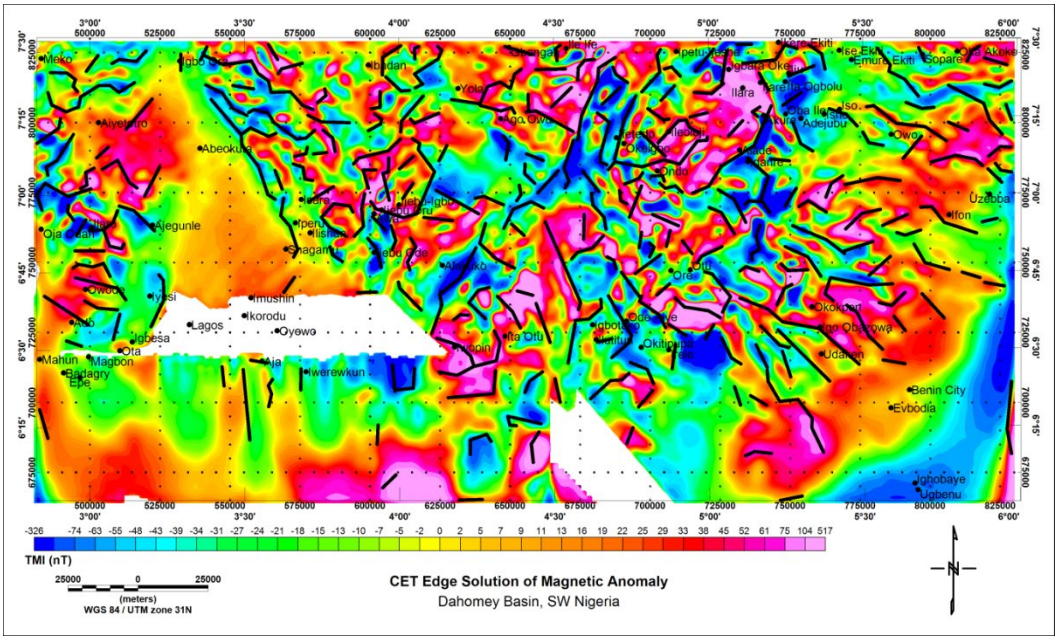

Figure 10. CET edge solution overlaid on magnetic data

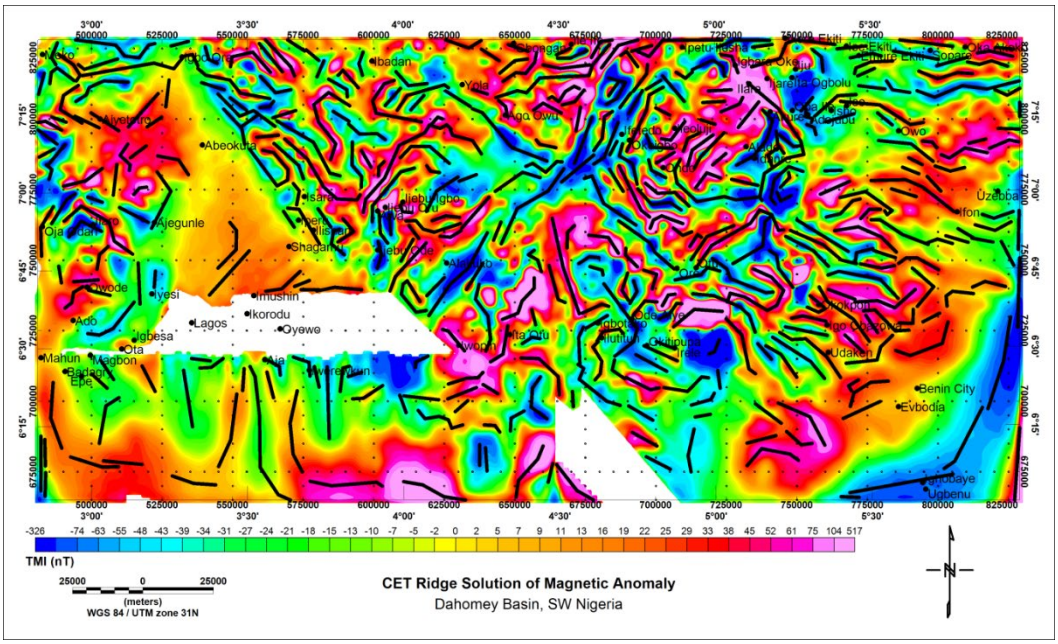

Figure 11. CET ridge solution overlaid on magnetic data

Traces in the western part of the study area trend mainly NW-SE. The central areas contain predominantly NE-SW trending traces. Lineaments that trend NW-SE dominate the eastern parts of the study area. The ridge solutions (Figure 11) are well developed in most parts of the study area. Here, the north-south trend of the basement structures is well defined, and the changing orientations across the study area are quite obvious. In addition, there are several basement fractures trending in various directions. The earlier interpreted NE-SW trending regional fracture through the middle of the study area is well defined on the CET maps, especially on the ridge model map (Figure 11). The trace along the peak of the negative anomaly (< -50 nT) in the south-east corner, coincide with the area reported to contain the Chain Fracture Zone [36,38,43].

4.8. Basement topography from magnetic data

The plot of depth solutions generated using the contact (SI = 0.0) model (Figure 12) presents depth values of 150 to 2500 m. The values appear to increase from north to south and from the middle of the map to the western and eastern parts. The basement topography grid (Figure 13) displays a wide variation in depths to basement, with the values ranging from 0 to -3500 m. The depth distribution shows a division of the study area into three geologic zones, which include the basement terrain (north), the Dahomey Basin (south-west) and the Niger Delta Basin (south-east). The plot of depth solutions generated using the dyke (SI = 1.0) model (Figure 14) presents depth values of < 500 to > 4500 m. The sedimentary terrain can be divided into two geologic zones, with the south-western part having depths > 2000 m, and the south-eastern side having depths generally greater than 1000 m. The basement topography grid (Figure 15) displays a rugged topography, with depth to basement values ranging from -150 to -5000 m. The depth distributions also show a division of the study area into three geologic zones. These include the basement terrain, the Dahomey Basin and the Niger Delta Basin. The basement terrain is the shallowest part of the study area, with depths < 1000 m. The Dahomey Basin is well highlighted and appears to be the deepest part of the study area. Depths to basement here range from -1500 m to -5300 m.

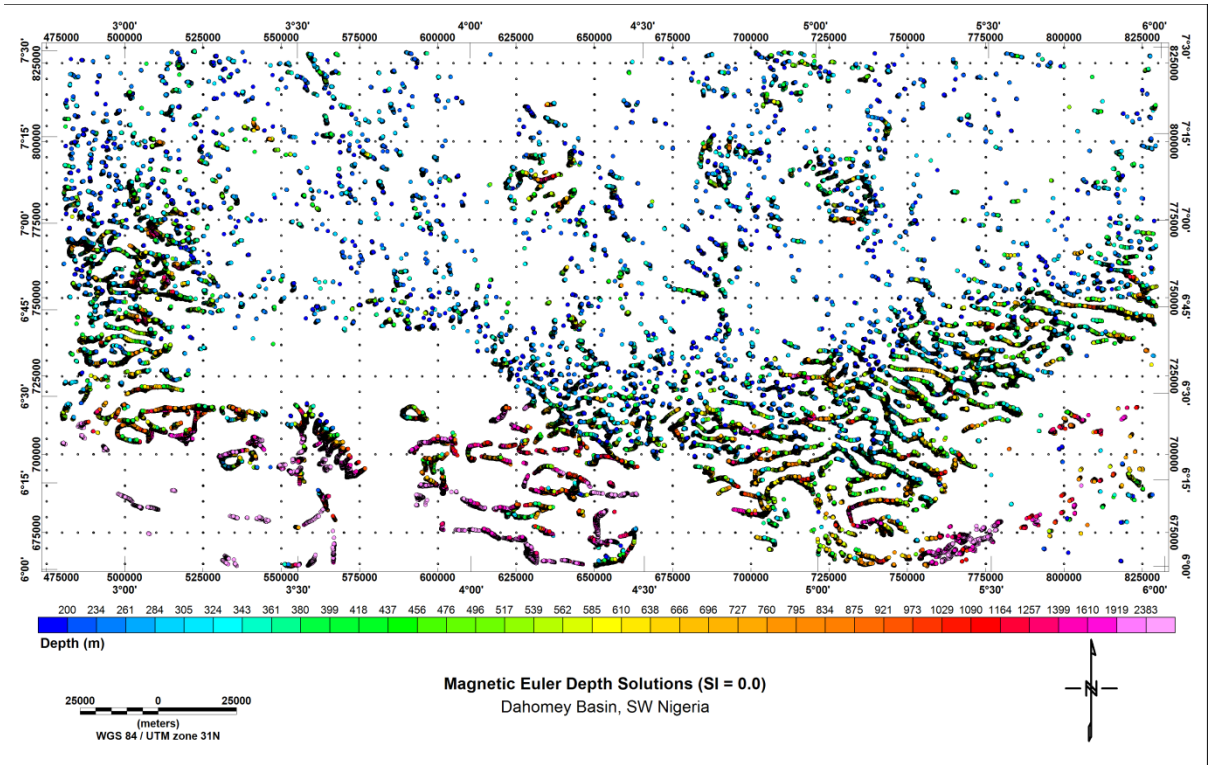

Figure 12. Depth to magnetic basement from magnetic data (SI=0.0)

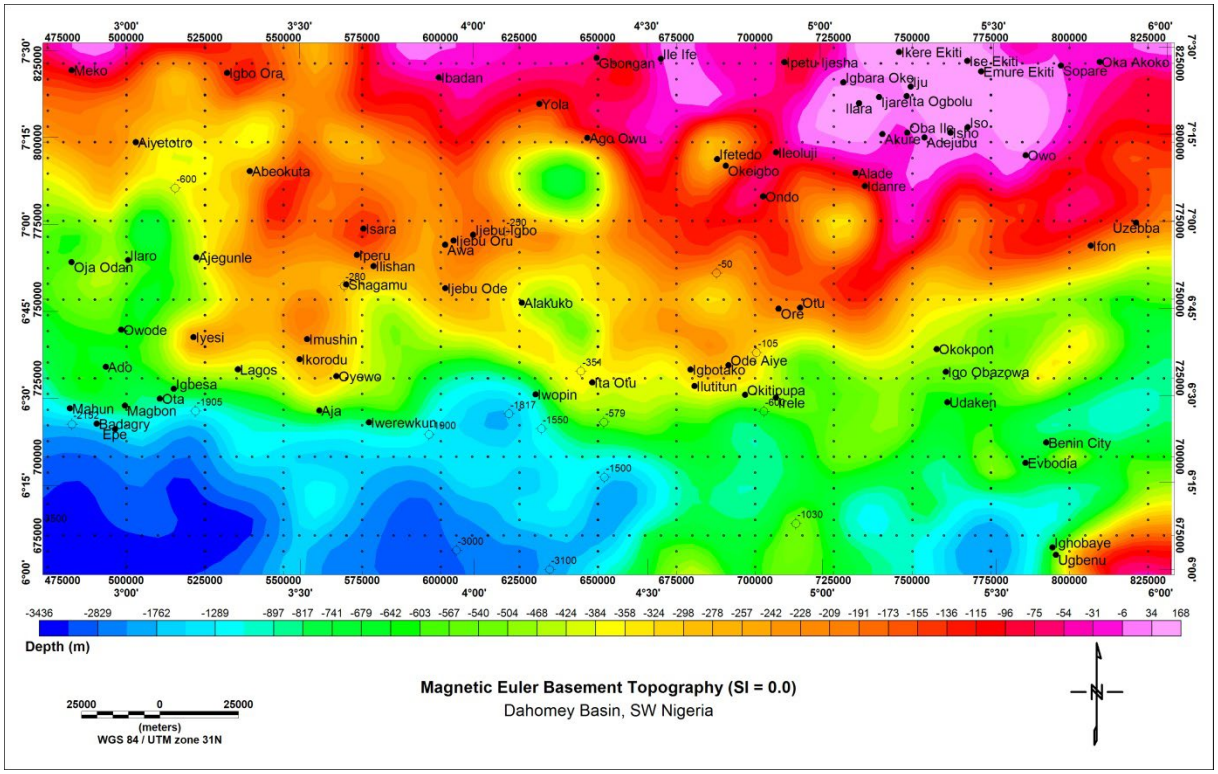

Figure 13. Basement topography from magnetic data (SI=0.0

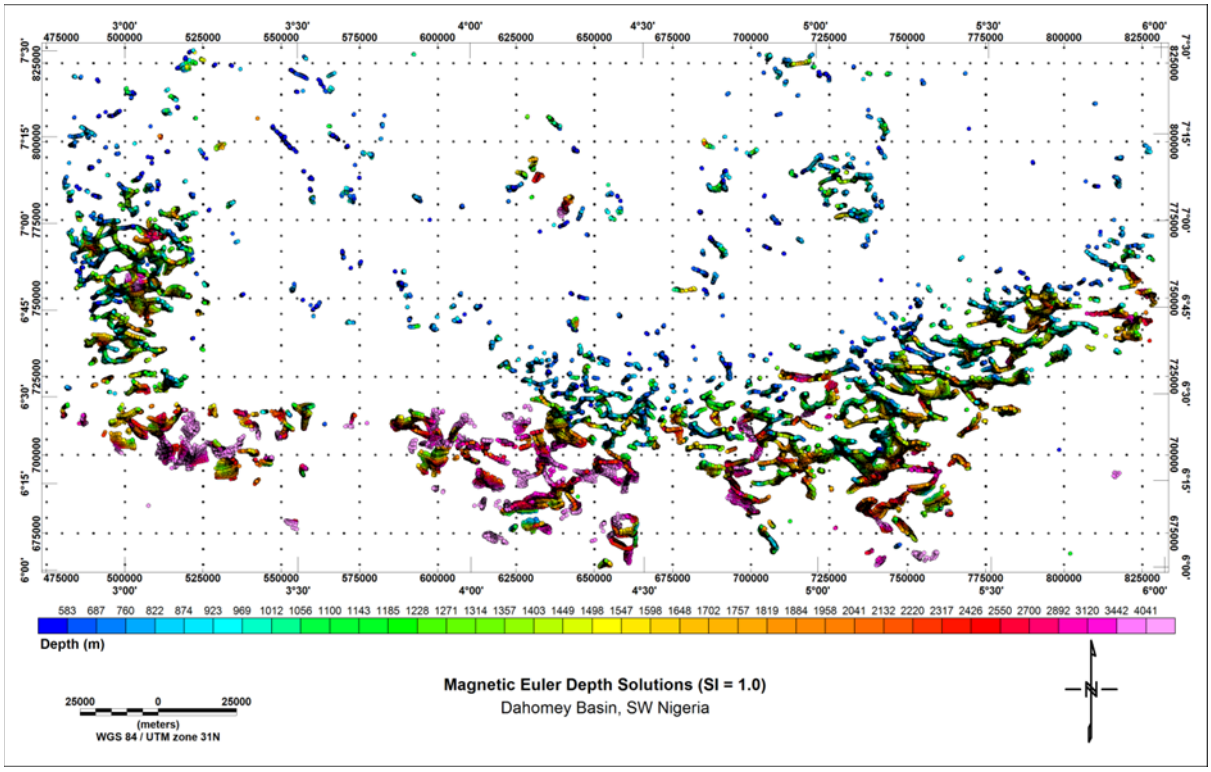

Figure 14. Depth to basement solutions from total field magnetic data (SI=1.0)

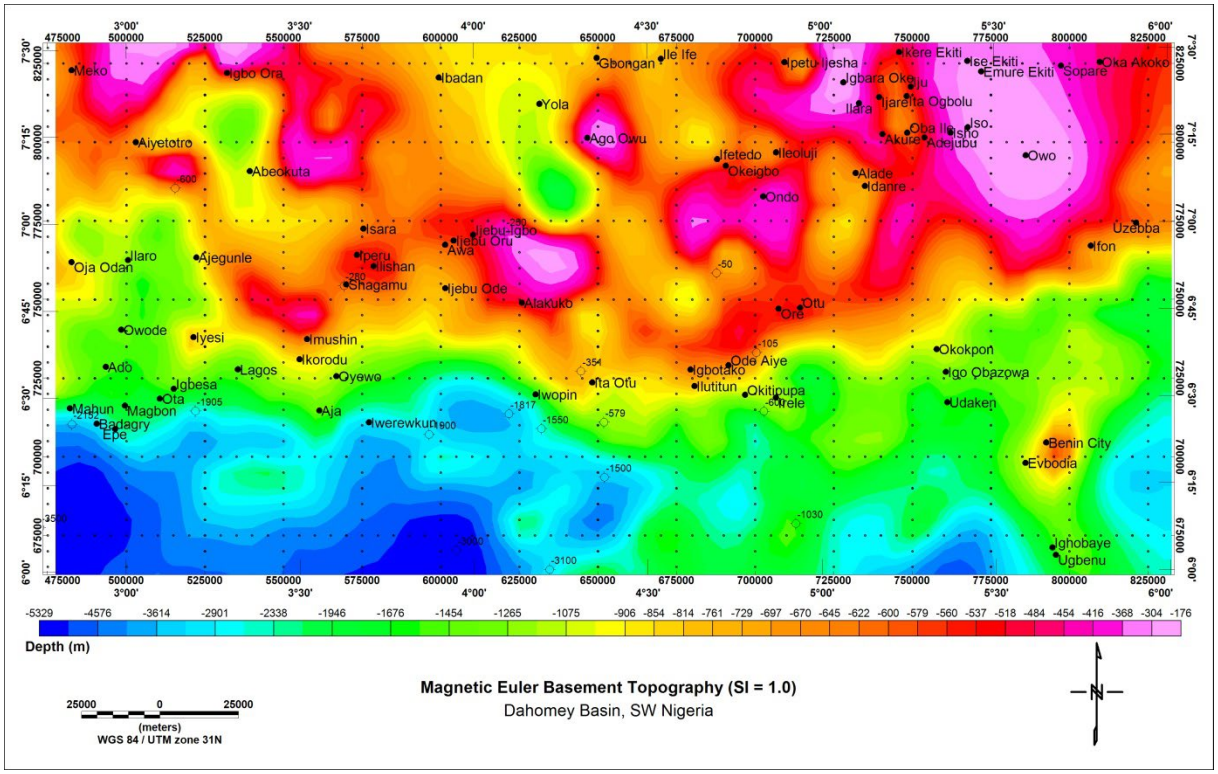

Figure 15. Basement topography from total field magnetic data (SI=1.0)

5. Discussion

Distinction of the study area into basement and sedimentary terrains was visible in the distribution of the total magnetic intensity data, in which the basement terrain is dominated by short wavelength anomalies, indicating shallow sources, while the sedimentary terrain is dominated by anomalies of relatively longer wavelengths, indicating deeper sources. The general geologic and structural trend in an approximate north-south direction [4,44-46]. Subsurface evidences on the underlying geology in the onshore and near-offshore parts of the eastern Dahomey Basin, shows the basin to be of undulating topography and the thicknesses of the sedimentary deposits vary markedly [36-37,39] and exceeds the minimum 3000 m thickness necessary for the formation and preservation of hydrocarbon in southern parts [4].

Data transformation and anomaly enhancements enables mapping of the geologic contacts, structural trends and delineation of the Dahomey Basin and Niger Delta Basin. The northern parts of the study area, coincides with the basement terrain of south-west Nigeria [35,47], while the southern parts of the study area coincides with the south-west Nigeria sedimentary terrain [8,47-48]. A NE-SW trending region of relatively high magnetic analytic signal amplitude (> 0.02 emu) separates the Dahomey Basin from the Niger Delta Basin. The location of this region around middle of the southern part of the study area, corresponds to the part of the study area reported in previous work to contain the basement uplift separating the Dahomey Basin from the Niger Delta Basin, known as the Okitipupa High [5,38].

Interpretations from the derivatives maps suggest that the geologic terrain is highly fractured, with significantly varying structural trends. This justifies the notion that the basement terrain and coastal basins of south-west Nigeria are highly fractured [39], with the basement rocks and overlying sediments bearing imprints of several episodes of tectonism [3,36,38,49-55]. In addition to the varying structural trends indicated the presence of several episodes of tectonic events, the Precambrian basement rocks have also been reported to be polycyclic in nature [56], which implies that several distinct rock units occur together and they can be differentiated on the bases of differences in age, mode of occurrences and tectonic records.

Lineament extraction using CET edge and ridge analyses add additional credence to the highly fractured nature of the underlying basement rocks. Regional fractures trending NE-SW were mapped in addition to several other small scale fractures, generally trending approximately north-south. In addition to fractures, the basement structures also consist of ridges and the interpreted NE-SW trending Okitipupa High (or Ridge), is the most discussed structural feature of the Nigerian sector of the Dahomey Basin [5,38,57]. The Okitipupa Ridge has also been described as the most important basement structure in the Nigerian sector of Dahomey Basin and it affects the structural styles of the overlying sediments [35].

The second result of Euler depth estimation with the contact model (SI = 0.0) differs in some ways from the first result of Euler depth estimation with the dyke model (SI = 1.0). Validation of the basement topography grids with depth information from boreholes drilled to basement reveals that the two solutions work differently for different parts of the study area. Basement depths from the contact model produces relatively shallower depths for the basement terrain, north of the study area, and the results obtained for the Dahomey Basin, southwest of the study area agrees with the borehole depths. However, the contact model produce basement depths that are shallower than the borehole depths, making the depth to basement values obtained unreliable. Basement depths from the dyke model produce depth values that agree more closely with the borehole depth, thereby making the result more reasonable. The dyke model however, produces depth values that are deeper than they should for the basement terrain and the Dahomey Basin.

It can be deduced from the basement topography maps that the basement terrain has an undulating topography. Depths to basement appear to increase from north to south, with the southwestern part appearing to be the deepest part of the study area. Depths to basement appears to increase to an initial value of 500 to 1000 m in the central parts of the study area, before increasing steeply to more than 3000 m in the Dahomey Basin, southwest of the study area. This suggests a step-wise subsidence of the crustal rocks, thereby supporting the notion that the Dahomey Basin is a sag basin [4]. In addition, the existence of basement rocks at more than 3000 m below the surface, also indicates that the Dahomey Basin contain the minimum 3000 m thickness of sediments deposits necessary for hydrocarbon formation. The presence of sufficient thickness of sediments for hydrocarbon formation has also been reported by several workers [40,58]. Traps within the Dahomey Basin are both structural and stratigraphic [36] and reactivation of the basement fractures has the potential to initiate formation of new trapping systems that can facilitate accumulation of hydrocarbon.

6. Conclusion

The basement terrain contains anomalies of relatively short wavelengths and high amplitudes, due to shallow source depths, while the sedimentary terrain exhibit smooth gradients. The additional distinction of the south-western Dahomey Basin from the south-eastern Niger Delta was made possible with the derivatives and analytic signal maps. Lineament analyses reveal that the subsurface basement is highly fractured, with the structures trending in varying directions. The fractures could have acted as hydrocarbon migration paths, considering the abundance of tar sands and oil-seeps around the basement/sedimentary transition zones, which has sediment depths of less than 2000 m. The presence of sediment thicknesses of up to 3000 m in the southern ends of the study area, suggests that there are untapped hydrocarbon deposits that could yet be discovered.

References

[1] Nton ME. Sedimentological and geochemical studies of rock units in the eastern Dahomey Basin, southwestern Nigeria. University of Ibadan, 2001.

[2] Adekoya JA, Kehinde-Phillips OO, and Odukoya AM. Geological distribution of mineral resources in Southwestern Nigeria. Nigerian Mining and Geosciences Society, 2003; 1–13.

[3] Osinowo OO, Akanji AO, and Olayinka AI. Application of high resolution aeromagnetic data for basement topography mapping of Siluko and environs , southwestern Nigeria. Journal of African Earth Sciences, 2014; 99: 637–651.

[4] OO Osinowo and AI. Olayinka Aeromagnetic mapping of basement topography around the Ijebu-Ode geological transition zone, Southwestern Nigeria. Acta Geod Geophys, 2013; 48: . 451–470.
[5] Omatsola ME, and Adegoke OS. Tectonic evolution and cretaceous stratigraphy of the Dahomey basin. Journal of Mining Geology, 1981; 18(1): 130–137.
[6] DE Falebita, OM Oyebanjo, and TR Ajayi A Geostatistical Review of the Bitumen Reserves of the Upper Cretaceous Afowo Formation Agbabu Area, Ondo State, Eastern Dahomey Basin, Nigeria. Pet Coal, 2014; 56(5): 572–581.
[7] Okosun EA. Review of the early Tertiary stratigraphy of Southwestern Nigeria. Journal of Mining and Geology, 1998; 34(1): 27–35.
[8] Obaje NG. Geology and Mineral Resources of Nigeria. Berlin: Springer, 2009.
[9] Isles DJ, and Rankin LR. Geological Interpretation of Aeromagnetic Data. 2018.
[10] Reeves C. Aeromagnetic Surveys: Principles, Practice and Interpretation. Washington D. C.: Geosoft, 2005.
[11] Blakely RJ, and Simpson RW. Locating edges of source bodies from magnetic or gravity anomalies. Geophysics, 1995; 51: 1494–1498.
[12] Feumoe ANS, Ndougsa-mbarga T, Manguelle-Dicoum E, and Fairhead JD. Delineation of tectonic lineaments using aeromagnetic data for the south-east Cameroon area. Geofizika, 2012; 29: 175–192.
[13] Ravat D. Reduction to Pole, Encyclopedia of Geomagnetism and Paleomagnetism. Springer, pp. 856–857, 2007.
[14] Baranov V, and Naudy H. Numerical calculation of the formula of reduction to the magnetic pole. Geophysics, 1964; 29(1): 67–79.
[15] Ansari AH, and Alamdar K. Reduction to the Pole of Magnetic Anomalies Using Analytic Signal. World Applied Sciences Journal, 2009; 7(4): 405–409.
[16] Blakely RJ. Potential theory in gravity and magnetic applications. Cambridge [England] ; New York: Cambridge University Press, 1996.
[17] Grant FS and Dodds J.MAGMAP FFT processing system development notes. Paterson Grant and Watson Limited., 1972.
[18] Luo Y, Xue DJ, and Wang M. Reduction to the Pole at the Geomagnetic Equator. Chinese Journal of Geophysics, 2010; 53(6): 1082–1089.
[19] Arkani-Hamed J. Differential Reduction-to-the-Pole of Regional Magnetic Anomalies. Geophysics, 1988; 53(12): 1592–1600.
[20] J. Arkani-Hamed, 'Differential Reduction to the Pole: Revisited.', Geophysics, vol. 72, no. 1, pp. L13–L20, 2007, doi: 10.1190/1.2399370.
[21] von Frese RRB, Hinze WJ, and Braile LW. Spherical earth gravity and magnetic anomaly analysis by equivalent point source inversion. Earth and Plan. Sci. Lett., 1981; 53: 69–83.
[22] Mendonca CA and Silva JCB. A stable truncated series approximation of the reduction-to-the-pole operator. Geophysics, 1993; 58: 1084–1090.
[23] Silva JCB. Reduction to the pole as an inverse problem and its application to low latitude anomalies. Geophysics, 1986; 51(2): 369–382.
[24] Rajagopalan S. Analytic signal vs. reduction to pole : Solutions for low magnetic latitudes. Exploration Geophysics, 2003; 34(4): 257–262.
[25] Keating P and Zerbot L. An improved technique for reduction to the pole at low latitudes. 1996; 61(1): 131–137.
[26] Wu JS and Wang JL. Improving the effect of reducing magnetic anomaly to pole in low magnetic latitude area by using directional high cut filter. Oil Geophysical Prospecting, 1992; 27(5): 670–677.
[27] Yao CL, Guan ZN, Gao ZD, Zhang X, and Zhang Y. Reduction to the pole of magnetic anomalies at low latitude with suppression filter. Chinese J. Geophys., 2003; 46(5): 690–696.
[28] Zhang XL. The least mean-square error filtering reduction to the pole of magnetic anomalies. Geophysical and Geochemical Exploration, 1995; 19(3): 200–211.
[29] Dentith MC, and Mudge ST. Geophysics for the mineral exploration geoscientist. Cambridge, United Kingdom: Cambridge University Press, 2014.
[30] Li X. Understanding 3D analytic signal amplitude. Geophysics, 2006; 71(2): L13-L16.
[31] Roest WR, Verhoef J, and Pilkington M. Magnetic interpretation using the 3-D analytic signal. Geophysics, 1992; 57(6): 116–125.
[32] Zhang C, Mushayandebvu MF, Reid AB, Fairhead JD, and Odegard ME. Euler deconvolution of gravity tensor gradient data, Geophysics, 2000; 65(2): 512–520.

[33] Mushayandebvu MF, van Driel P, Reid AB, and Fairhead JD. Magnetic source parameters of two-dimensional structures using extended Euler deconvolution, Geophysics, 2013; 78(3): 814–823.
[34] Reid AB, Allsop JM, Millet AJ, and Somerton IW. Magnetic interpretation in three dimensions using Euler deconvolution. Geophysics 55, 80–91. Geophysics, 1990; 55: 80–91.
[35] Avbovbo AA. Basement geology in the sedimentary basins of Nigeria. Geological Society of America, 1980; 8: 323–327.
[36] Brownfield ME and Charpentier RR. Geology and Total Petroleum Systems of the Gulf of Guinea Province of West Africa. Geological Survey Bulletin, 2006; 2207.
[37] Kaki C, Almeida GAF, Yalo N, and Amelina S. Geology and Petroleum Systems of the Offshore Benin Basin (Benin)', Oil and Gas Science and Technology, 2013; 68(2): 363–381, 2013.
[38] Ola PS and Olabode SS. mplications of horsts and grabens on the development of canyons and seismicity on the west Africa coast. J. of African Earth Sciences, 2018; 140:282-290.
[39] Osinowo OO and Olayinka AI. Very low frequency electromagnetic (VLF-EM) and electrical resistivity (ER) investigation for groundwater potential evaluation in a complex geological terrain around the Ijebu-Ode transition zone , southwestern Nigeria. Journal of Geophysics and Engineering, 2012; 9: 374–396.
[40] Whiteman AJ. Nigeria: Its petroleum geology, resources and potential. London: Graham and Trottan, 1982.
[41] Reid AB, Ebbing J, and Webb SJ. Avoidable Euler Errors – the use and abuse of Euler deconvolution applied to potential fields', Geophysical Prospecting, 2014; 62(5): 1162–1168.
[42] Stavrev P. and Reid AB. Euler deconvolution of gravity anomalies from thick contact/fault structures with extended negative structural index. Geophysics, 2010; 75: 151–158.
[43] Oluyide PO and Udoh AN. Preliminary comments on the fracture systems of Nigeria', in National seminar on earthquakes in Nigeria, 1989, pp. 97–109.
[44] Oladele S, Ayolabi EA, and Olobaniyi SB. Structural Features of the Benin Basin , Southwest Nigeria Derived from Potential Field Data. Journal of Mining and Geology, 2015; 51(2): 151–163.
[45] Opara AI. Second vertical derivatives and trend surface analysis of the aeromagnetic data over part of the Benin Basin , Nigeria. Global Journal of Geological Sciences, 2011; 9(1): 19–26.
[46] Opara AI, Ekwe AC, Okereke CN, Oha IA, and Nosiri OP. Integrating Airborne Magnetic and Landsat Data for Geologic Interpretation over part of the Benin Basin , Nigeria. The Pacific Journal of Science and Technology, 2012; 13(1): 556–571.
[47] Kogbe CA. Geology of Nigeria, Second. Jos: Rockview Nig. Ltd., 1989.
[48] NGSA, Nigerian Geological Survey Agency: Geological Map of Nigeria. Ministry of Mines and Steel Development, Abuja, Nigeria, 2005.
[49] Akinmosin A, Omosanya K, Ariyo S, Folorunsho AF, and Aiyeola SO. Structural Control for Bitumen Seepages in Imeri, Southwestern Nigeria', International Journal of Basic & Applied Sciences,2011; 11(93): 118601–4949.
[50] Burke KCB, Dessauvagie TFJ, and Whiteman AJ. The opening of the Gulf of Guinea and the geological history of the Benue Depression and Niger Delta. Nature Phys. Sci., 1971; 233(38): 51–55.
[51] Ikhane PR, Omosanya KO, Akinmosin AA, and Odugbesan AB. Electrical Resistivity Imaging (ERI) of Slope Deposits and Structures in Some Parts of Eastern Dahomey Basin. Journal of Applied Sciences, 2012; 12(8): 716–726.
[52] McGregor DS, Robinson J, and Spear G. Play fairways of the Gulf of Guinea transform margin. in Petroleum Geology of Africa—New Themes and Developing Technologies: Geological Society, T. J. Arthur, D. S. MacGregor, and N. R. Cameron, Eds. London: Special Publication 207, 2003, p. 289.
[53] McCurry P. The geology of the Precambrian to lower Palaeozoic rocks of Northwestern Nigeria.', in Geology of Nigeria, C. A. Kogbe, Ed. Lagos: Elizabeth Publishing Company, 1976, pp. 115–150.
[54] Odeyemi I. A review of the orogenic events in the Precambrian basement of Nigeria, West Africa.', Geologische Rundschau, 1981; 70: 897-909.
[55] Oyinloye AO. Genesis of the Iperindo gold deposit, Ilesha schist belt, Southwestern Nigeria.', University of Wales, Cardiff, U.K., 1992.
[56] Ajibade AC, Woakes M, and Rahaman MA. Proterozoic crustal development in the Pan-African regime of Nigeria. in Proterozoic Lithospheric Evolution, vol. 17, A. Kröner, Ed. American Geophysical Union, 1987, pp. 259–270.
[Online]. Available: https://doi.org/10.1029/GD017p0259.

[57] Nton ME, Ikhane PR, and Tijani MN. Aspect of Rock-Eval Studies of the Maastrichtian-Eocene Sediments from Subsurface , in the Eastern Dahomey Basin Southwestern Nigeria', European Journal of Scientific Research, vol. 25, no. 3, pp. 417–427, 2009.
[58] Billman HG. Offshore stratigraphy and paleontology of the Dahomey (Benin) Embayment, West Africa. Nigerian Association of Petroleum Explorationists Bulletin, 1992; 7(2): 121–130.

To whom correspondence should be addressed: Dr. Michael Oluwaseyi Falufosi, Pan African University Life and Earth Sciences Institute, University of Ibadan, Ibadan, Nigeria, E-mail: michael.falufosi@gmail.com